4th Intercontinental Geoinformation Days

igd.mersin.edu.tr

Exploring the spatial distribution and intensity of Urban Heat Islands (UHI) in Ardabil city

Iraj Teymouri *[1]

[1]*University of Tabriz, Planning & Environmental Studies, Urban Planning and Geography, Tabriz, Iran*

Keywords
Land surface temperature
Urban Heat Island
Water Bodies
Thermal effect

Abstract

The first purpose of this paper was, calculating land surface temperature (LST) and exploring the spatial distribution of UHI in Ardabil city which was investigated using Land sat 8 OLI/TIRS images for summer and winter of 2019. The second purpose was exploring the thermal effects of Shourabil Lake on surrounding area. The results showed, high temperature is most widespread in suburban areas especially in south, south west, west and north west rather than central parts of the city. Also, the results showed the maximum average temperature in imaging time of winter was 18 ºC, recorded from industrial areas and the maximum average temperature in imaging time of summer was 27 ºC recorded from military and Festival site. The average temperature of water body in summer and winter were 17 ºC and 16 ºC respectively. According to the results thermal effects of the Shourabil lake was limited to 200m, the resultant correlation model for LST and distance to lake based on the calculated R (0.896, 0.988, 0.950) demonstrate a strong correlation, notably the regression could estimate the thermal variation around the lake in this distance.

1. Introduction

Urban Heat Island (UHI) is one of the more serious impacts of urbanization on urban climate (Hirano & Fujita, 2012).Thermal properties of different materials, evaporation of surfaces and reduced ability of the released infrared (IR) radiation to escape from urban structures into the atmosphere have also evolved significant causes of UHI(R. P. Gupta, n.d.; Mathew, Sreekumar, Khandelwal, & Kumar, 2019).The UHI effect can be reduced by making changes in built form, material selection, and land use proportion in cities in order to raise the albedo and cool the surrounding(Nastran, Kobal, & Eler, 2019). Land surface temperature (LST) varies significantly across different land cover classes (Ren et al., 2016; Susca et al., 2018). LST is usually higher in built-up areas, such as those for residential and industrial land use, and bare surfaces(Shaker, Altman, Deng, Vaz, & Forsythe, 2019) It is lower in water bodies like ponds, lakes and river which have a significant role in reducing the UHI (Hathway & Sharples, 2012). Also vegetation, as a key instrument of mitigating urban heat island, influences the cooling process due to evaporative cooling and shading surfaces which absorb short-wave radiation (Kolokotroni & Giridharan, 2008).During last years' significant research efforts have been performed to evaluate the urban heat island phenomenon and the mitigating effects of water bodies and green space. (Cai, Han, & Chen, 2018), indicate that the cooling effect of water bodies can reach one kilometer (horizontal distance).(Nakayama & Hashimoto, 2011), highlighted that effective management of water resources would be powerful for ameliorating the heat island.(Amani-Beni, Zhang, Xie, & Xu, 2018), found that the for every 1000 m increase in distance from the river, the UHI decreased by 0.6 ºC to 3 ºC depending on season. Also(Xiao, Dong, Yan, Yang, & Xiong, 2018), found that the cooling and humidifying effect of large green spaces was more obviouse and stabl, and the cooling effect of small green spaces was more was more variable. (Hathway & Sharples, 2012) showed that the urban form on the river bank influenced the levels of cooling felt away from the river bank. Also (Giridharan & Kolokotroni, 2009), showed that the winter climate control modes have the same correlation, indicating that most change in outdoor temperature are caused by climate factors and not the on-site variables.

The review of previous studies pointed out mitigation effect of water bodies and green space in urban heat

* **Corresponding Author**

*(iraj-teymuri@tabrizu.ac.ir) ORCID ID 0000 – 0002 – 3168 – 5583

Cite this study

Teymouri, I. (2022). Exploring the spatial distribution and intensity of Urban Heat Islands (UHI) in Ardabil city. 4th Intercontinental Geoinformation Days (IGD), 37-42, Tabriz, Iran

island. The purpose of this study is to investigate the urban heat island and the mitigation effect achieved by water body during February and June. According to foregoing the present study was carried out to follow 3 objectives: (1) the study of LST in Ardabil city using Land Sat 8 OLI/TIRS satellite image during the summer and winter of the year 2019, (2) Calculating of UHI in the city, (3) analysing the effect of Shourabil lake on the surrounding achieved temperature.

2. Method

In this study, to evaluate the UHI and influenced area of the city, the satellite images of land sat 8 OLI/ TIRS (thermal band 10) were used The metadata of images were featured in Table 1.

In order to compute the LST, the thermal band digital number (DN) is numerically converted to radiometric scale using Eq. (1).

Eq. (1) is used for converting DN to radiance in Landsat 7 ETM image:

$$L_\lambda = \left(\frac{LMAX_\lambda - LMIN_\lambda}{QCALMAX - QCALMIN}\right) * (QCAL - QCALMIN) + LMIN_\lambda$$

Where
L_λ= the cell value as the radiance
QCAL=digital number
$LMIN_\lambda$= spectral radiance scales to QCALMIN
$LMAX_\lambda$= spectral radiance scales to QCALMAX
QCALMIN=the minimum quantized calibrated pixel value (typically =1)
QCALMAX+ the maximum quantized calibrated pixel value (typically =255)

The value of $LMIN_\lambda$ and $LMAX_\lambda$extracted from the header file of landsat images are 0.10033 and 22.00180 respectively (Table.1)

Table 1. Metadata of satellite image

Variable	description	value	Image, DATE_ACQUIRED	Scene center time
K1	Thermal Constants Band 10	774.8853		
K2		1321.0789	2019-02-26	07:25:32
Lmax	Maximum and minimum values of Radiance, Band 10	22.00180	2019-06-18	07:25:41
Lmin		0.10033		
QCALMAX	Maximum and minimum values of Quantize Calibration, Band 10	65535		
QCALMIN		1		
Oi	Orrection value, Band 10	0.29		

Converting radiance to brightness temperature

After calculating spectral radiance (L_λ), the images were computed for their brightness temperature using either Planck's radiance function for temperature (Weng et al.,2004) or the approximation formula shown in Eq (3).

Where T is the effective at sensor brightness temperature in Celsius, k_1 is calibration constant (in kelvin), k_2 is the calibration constant (Watts/$[m^2 * sr * \mu m]$), and Ln is the natural logharithem. Values of , $k_1$and k_2 for images are shown in Table 2.

$$T_{°C} = \frac{k_2}{Ln(\frac{k_1}{L} + 1)} - 273.15$$

Table 2. UHI Category

0-0.2	0.2-0.4	0.4-0.6	0.6-0.8	0.8-1
Very Low	Low	Moderate	High	Very High

LST retrieved from each image of the studied period using the Eq. (4): (Weng & Lu, 2008).

$$LST = \frac{BT}{1 + W * \left(\frac{BT}{P}\right) * Ln(\varepsilon)}$$

W is the effective band wave length (11.475 μm), $P = h * \frac{c}{s}(1.438 * 10^{2-}mK)$, h= Planck's constant, c= velocity of light, s= Boltzman constant ($1.38 * 10^{23-}j/k$) and ε is land surface emissivity.

Land surface emissivity (ε) was estimated based on NDVI thresholds method as proposed by Sorbrino et al. (2004) as follows:

Normalized Differential Vegetation Index (NDVI) is calculated using the equation

$$\text{NDVI} = \frac{(NIR - VIS)}{(NIR + VIS)}$$

Where NIR and VIS are the near-infrared and visible light bands, respectively

If NDVI<0.15, then the pixel is considered as bare soil and the mean emissivity value used in this study was 0.97

if, NDVI>0.62

These kinds of pixels are considered as fully vegetated, and then a constant value for emissivity is assumed typically of 0.99

In the case of 0.15<NDVI<0.62

Is this case emissivity is calculated according to Eq. (6).

$$\varepsilon = \varepsilon_v P_v + \varepsilon_s(1 - P_v)$$

Where ε_v is the vegetation emissivity and $\varepsilon_s$is the soil emissivity. P_v is the proportion of vegetation obtained according to Eq. (7) (Sobrino et al., 2004).

$$P_v = \left(\frac{NDVI - NDVI_{min}}{NDVI_{max} + NDVI_{min}}\right)^2$$

Where $NDVI_{max}$=0.62 and $NDVI_{min}$=0.15

based on the Eq. (8) we construct the UHI intensity index;

$$UHI_{ii} = \frac{LST_{Max} - LST}{LST_{max} - LST_{min}}$$

Then, achieved data were classified based on defined interval method with intervals of 0.2. in this method we obtained 5 classes, which categorized as Table 2.

2.2. Statistical modeling methodology

The approach behind this study bass on assumption that water body has mitigation effect on LST, thus the relation ship between LST and distance to Shourabil-Lake were correlated using with Pearson Correlation test in SPSS 25. Further investigation of possible influence of Shourabil - Lake on LST has been explored by profile tools in ArcGIS10.2 3D analyst and Linear Regression Model in SPSS. The linear regression model is estimated with Eq. (9):

$$LST = \alpha + \beta x$$

2.3. Spatial analysis

This study used Land use map as a Zone data feature in ArcGIS. 10.2 for calculation of descriptive statistic such as, Mean, Maximum, Minimum of obtained LST for every land use type.

Finally, the temperature of the city was calculated based on Eq. (10)

$$total = \sum_{i=1}^{n} LST_{LU_i} * W_{LU_i}$$

Where; W_{LU_i} is;

$$W_{LU_i} = \frac{Area_{Lu_i}}{\sum Area_{Lu}}$$

3. Results

To find the relationship between LST and land use, the thermal values of each land use class was obtained by overlaying a LST map with Land-use map in ArcGIS 10.2- Zonal Analysis Tool. The same was used for obtaining UHI. The LST (mean, minimum and maximum) values for various land use type for each of the images is summarized in Table 3. According to the LST map, surface temperature varied between 11ºC and 36 ºC at the imaging time in June. As Table 3. shows, the lowest average temperature was 15 ºC related to parking area and the maximum average temperature was 27 ºC recorded from military and Festival site, also average temperature of water body and residential areas were low, the calculated temperature for these areas were, 17 ºC. The calculated temperature for industrial site was high, 26 ºC. based on calculation the average temperature of the city in the imaging time of June was 20.6 ºC. according to the table. 2. the UHIII in the industrial, police station and festival site were high and the lowest UHIII related to parking, water bodies, residential, cultural, sanitation and treatment areas. The UHIII in the other type of land uses were moderate, specially in bare lands. Finally, the UHIII of the city was low, 0.39, which refer to a cool weather in the imaging time.

In this paper for exploring the Shourabil Lake's effect on surrounding area, we used correlation test and regression analysis, the explanatory variable was distance to lake which extracted by line profile in ArcGIS 10.2- 3d Analyst tools, Fig 2. demonstrate the position of line profiles.

Table 3. Model summery

		Festival Site	Military site	industrial	Green Space	Agricultur e	Facilities	Education al	Grass	Bare lands	Transport	Sport	Tourism	Orchard	Administr ative under construct.	Commerci al &	Sanitation &	Cultural site	Other	Residentia l	water body	Parking	Total
June 2019	Mean	27	27	26	25	24	24	24	23	23	23	22	22	22	22	22	20	19	19	17	17	15	206
	Min	26	15	15	14	17	14	13	16	14	15	15	15	15	14	15	14	13	17	12	13	14	13.3
	Max	29	33	31	32	31	30	33	29	32	29	29	28	30	31	27	29	25	22	29	29	17	36.3
	Mean UHI	0.68	0.67	0.64	0.60	0.54	0.54	0.52	0.50	0.50	0.47	0.47	0.46	0.45	0.44	0.44	0.41	0.35	0.33	0.33	0.24	0.21	0.39
	UHII	H	H	H	M	M	M	M	M	M	M	M	M	M	M	M	M	L	L	L	L	V L	L
February 2019	Mean	16	17	18	16	17	16	15	13	13	14	14	15	14	14	13	13	11	12	11	9	16	9	124
	Min	14	7	6	6	9	9	5	6	5	7	7	7	7	6	6	5	7	5	10	4	10	8	5.4
	Max	17	22	24	21	26	20	21	18	22	20	20	18	17	21	19	22	16	20	12	20	25	10	214
	Mean UHI	0.43	0.48	0.51	0.43	0.48	0.43	0.42	0.35	0.34	0.37	0.37	0.39	0.37	0.37	0.35	0.33	0.28	0.29	0.28	0.19	0.44	0.17	0.31
	UHII	M	M	M	M	M	M	M	L	L	L	L	L	L	L	L	L	L	L	L	VL	M	VL	L
	Area M^2	53100	11502	99630	32085	27594	13860	24012	25650	91431	32580	26010	70200	39150	69570	67500	12483	24390	21060	13500	17343	27198	5400	437.03

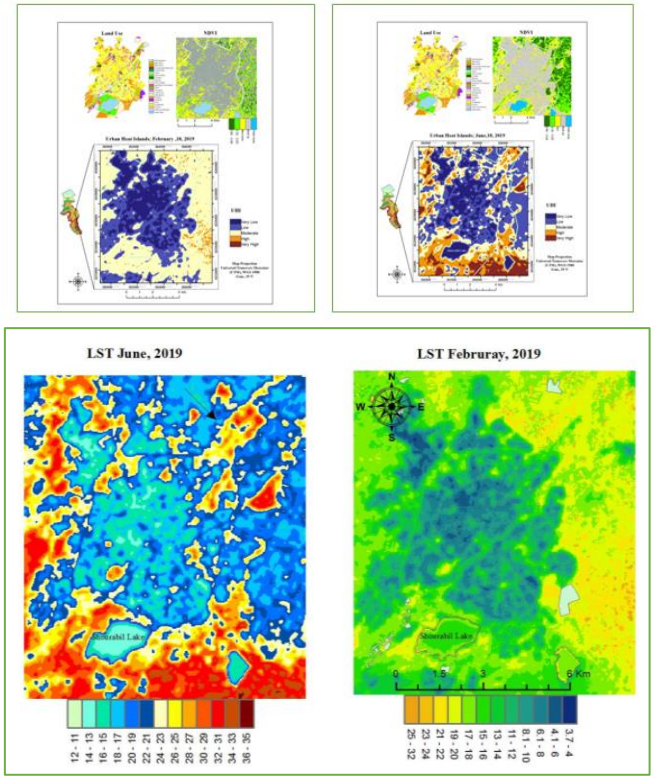

Fig.1. UHI and Land Surface Temperature

The resultant correlation model for LST and distance to lake based on the calculated R, demonstrate a strong correlation, notably the regression could estimate the thermal variation around the lake. According to the analysis, due to the achieved r (0.896, 0.988, 950) and Beta, the lake's impact on temperature are positive, which means in this class the lake's temperature warms up the surrounding area, based on the obtained R (-0.997, -0.700, -0.857) and Beta for class 2, distance from lake shows negative impact on temperature. That means the temperature after certain distance to lake tends to reduce.

Fig.2. Position of the profiles, profile l,2,3-left to right a. February, 2019

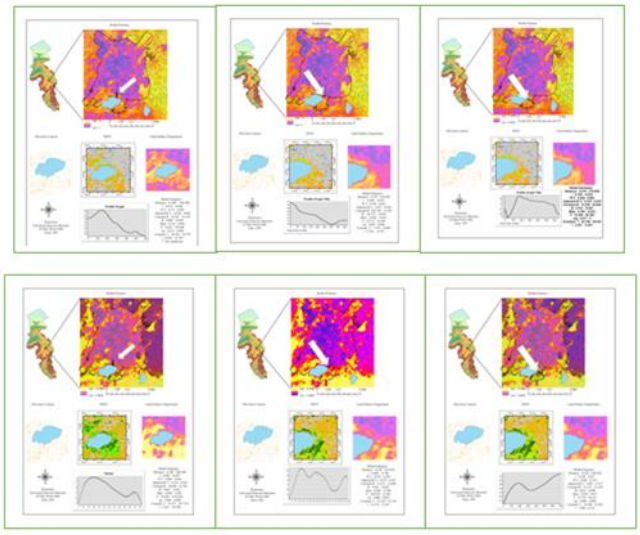

Table 4. The model summery for Summer, June 2019

		Distance	R	R^2	AdjR^2	Constant B	B	Beta	F	Constant T	T	Sig
Profile 1	Class 1	0-180	0.896	0.803	0.764	18.689	0.025	0.896	20.389	31.073	4.515	0.006
	Class2	180-400	-0.997	0.994	0.993	24.702	-0.013	-0.997	1332.820	197.724	-36.508	0.000
Profile 2	Class 1	0-210	0.988	0.976	0.972	14.133	0.034	0.988	240.916	52.250	15.521	0.000
	Class2	210-650	-0.700	0.490	0.451	21.028	-0.005	-0.700	12.482	32.142	-3.533	0.004
Profile 3	Class 1	0-210	0.950	0.903	0.887	21.127	0.025	0.950	55.739	52.940	7.466	0.000
	Class2	210-650	-0.857	0.734	0.715	21.350	0.008	0.857	38.615	34.262	6.214	0.000

4. Discussion

Different type of urbans can cause the formation of different forms of heat islands. this study highlighted that the residential areas of the Ardabil city were cooler than the surrounding areas. In other words, Lower LST values tended to be distributed in the center of study area while the highest LST values were scattered around the city. On the whole, only 5% of Ardabil area suffer from High values of UHI, on the other hand the UHI values for 46% of the city area were low. Similarly, (Shirani-bidabadi, Nasrabadi, Faryadi, Larijani, & Shadman Roodposhti, 2019) suggested that down town area in Isfahan city experienced lower temperature than the suburban areas during day time. In the case of Ardabil this can be partly due to existence of bare lands in suburban areas, especially in the south and south west, which mostly absorb sunlight than reflecting it and that leads to a higher temperature in suburban than downtown. Also the same results were obtained by (Lazzarini, Marpu, & Ghedira, 2013), highlighted that down town area in some other aired and semi-arid cities such as Abu Dhabi, Kuwait City, Riyadh, Las Vegas, Phoenix, and Biskra experienced lower temperature than suburban areas during the day time. (Bokaie et al., 2016), state that industrial area in Tehran suffer from high level of LST during day time. Our results show a similar finding which the average temperature of industrial areas was high, especially in the imaging time of winter, the calculated temperature for industrial areas were about 18 ºC, which is 6 ºC higher than the mean temperature of the city. Also similar results highlighted by (El-Hattab, Amany, & Lamia, 2018), According to the results, because of surrounding topography and Land use type, the thermal effects of Shourabil lake was limited to a short distance. Different to (Moyer & Hawkins, 2017) this study showed that after certain distance from the lake temperature tends to reduce; case profile 1, profile 3 in February 26Th 2019, and all cases of summer. According to the analysis, due to the achieved r (0.896, 0.988, 950) and Beta, the lake's impact on temperature is positive, which means in class1 the lake warms up the surrounding area. The reduction of temperature after 200 m was variable based on the nature of topography and land cover. Similarly (N. Gupta, Mathew, & Khandelwal, 2019), highlighted that the temperature in the river bank of Sabarmati was low within 200 m of the river and shows a sharp ascent there onwards. Also, the results which were obtained by (Wu & Zhang, 2019), it can be said that various factors affect the thermal impacts of water bodies, in the case of Shourabil lake, the rising temperature in the surrounding areas especially in the north, west and south of the lake may be due to the presence of bare lands. In the east of the lake-built area alongside the green space cause a decrease in temperature

5. Conclusion

The research concerning distribution of LST in Ardabil city for two different time during 2019. In order to determine the general distribution of UHI in Ardabil regarding to land use type the land sat 8 images were used. Due to the geographical position of the city and the imaging time, residential areas of the Ardabil city were cooler than the surrounding areas. As the results showed, Lower LST values tended to be distributed in the center of city while the highest LST values were scattered around the study area. The results highlighted that the average temperature of industrial areas in the imaging time of winter were high. Also, we explored the thermal effect of Shourabil Lake on surrounding area, our study indicated that the thermal effect of the lake is limited to a short distance from lake, the study showed during imaging time because of surrounding land use type the temperature after 200 m onward tends to reduce. This study opens an opportunity and necessity for further research about the spatial pattern recognition of UHI and LST in Ardabil. There is need for more in-depth analysis of a selected city and thermal effect of water bodies.

References

Amani-Beni, M., Zhang, B., Xie, G. di, & Xu, J. (2018). Impact of urban park's tree, grass and waterbody on microclimate in hot summer days: A case study of Olympic Park in Beijing, China. *Urban Forestry and Urban Greening*, *32*(January), 1–6. https://doi.org/10.1016/j.ufug.2018.03.016

Bokaie, M., Zarkesh, M. K., Arasteh, P. D., & Hosseini, A. (2016). Assessment of Urban Heat Island based on the relationship between land surface temperature and Land Use/ Land Cover in Tehran. *Sustainable Cities and Society*, *23*, 94–104. https://doi.org/10.1016/j.scs.2016.03.009

Cai, Z., Han, G., & Chen, M. (2018). SC. *Sustainable Cities and Society*. https://doi.org/10.1016/j.scs.2018.02.033

Centre, S. (n.d.). *Population based on the National Population and Housing Census, 2016*.

Dwivedi, A., & Mohan, B. K. (2018). Impact of green roof on micro climate to reduce Urban Heat Island. *Remote Sensing Applications: Society and Environment*, *10*(February), 56–69. https://doi.org/10.1016/j.rsase.2018.01.003

El-Hattab, M., Amany, S. M., & Lamia, G. E. (2018). Monitoring and assessment of urban heat islands over the Southern region of Cairo Governorate, Egypt. *Egyptian Journal of Remote Sensing and Space Science*, *21*(3), 311–323. https://doi.org/10.1016/j.ejrs.2017.08.008

Giridharan, R., & Kolokotroni, M. (2009). Urban heat island characteristics in London during winter. *Solar Energy*, *83*(9), 1668–1682. https://doi.org/10.1016/j.solener.2009.06.007

Gupta, N., Mathew, A., & Khandelwal, S. (2019). The Egyptian Journal of Remote Sensing and Space Sciences Analysis of cooling effect of water bodies on land surface temperature in nearby region : A case study of Ahmedabad and Chandigarh cities in. *The Egyptian Journal of Remote Sensing and Space Sciences*, *22*(1), 81–93. https://doi.org/10.1016/j.ejrs.2018.03.007

Gupta, R. P. (n.d.). *Remote Sensing Geology*.

Hathway, E. A., & Sharples, S. (2012). The interaction of rivers and urban form in mitigating the Urban Heat Island effect: A UK case study. *Building and Environment*, *58*, 14–22. https://doi.org/10.1016/j.buildenv.2012.06.013

Hirano, Y., & Fujita, T. (2012). Evaluation of the impact of the urban heat island on residential and commercial energy consumption in Tokyo. *Energy*, *37*(1), 371–383. https://doi.org/10.1016/j.energy.2011.11.018

Jato-Espino, D. (2019). Spatiotemporal statistical analysis of the Urban Heat Island effect in a Mediterranean region. *Sustainable Cities and Society*, *46*(October 2018), 101427. https://doi.org/10.1016/j.scs.2019.101427

Kolokotroni, M., & Giridharan, R. (2008). Urban heat island intensity in London: An investigation of the impact of physical characteristics on changes in outdoor air temperature during summer. *Solar Energy*, *82*(11), 986–998. https://doi.org/10.1016/j.solener.2008.05.004

Lazzarini, M., Marpu, P. R., & Ghedira, H. (2013). Temperature-land cover interactions: The inversion of urban heat island phenomenon in desert city areas. *Remote Sensing of Environment*, *130*, 136–152. https://doi.org/10.1016/j.rse.2012.11.007

Levermore, G., Parkinson, J., Lee, K., Laycock, P., & Lindley, S. (2018). The increasing trend of the urban heat island intensity. *Urban Climate*, *24*, 360–368. https://doi.org/10.1016/j.uclim.2017.02.004

Mathew, A., Sreekumar, S., Khandelwal, S., & Kumar, R. (2019). Prediction of land surface temperatures for surface urban heat island assessment over Chandigarh city using support vector regression model. *Solar Energy*, *186*(March), 404–415. https://doi.org/10.1016/j.solener.2019.04.001

Mirzaei, P. A., Haghighat, F., Nakhaie, A. A., Yagouti, A., Giguère, M., Keusseyan, R., & Coman, A. (2012). Indoor thermal condition in urban heat Island - Development of a predictive tool. *Building and Environment*, *57*, 7–17. https://doi.org/10.1016/j.buildenv.2012.03.018

Moyer, A. N., & Hawkins, T. W. (2017). River effects on the heat island of a small urban area. *Urban Climate*, *21*, 262–277. https://doi.org/10.1016/j.uclim.2017.07.004

Nakayama, T., & Hashimoto, S. (2011). Analysis of the ability of water resources to reduce the urban heat island in the Tokyo megalopolis. *Environmental Pollution*, *159*(8–9), 2164–2173. https://doi.org/10.1016/j.envpol.2010.11.016

Nastran, M., Kobal, M., & Eler, K. (2019). Urban heat islands in relation to green land use in European cities. *Urban Forestry and Urban Greening*, *37*(January 2018), 33–41. https://doi.org/10.1016/j.ufug.2018.01.008

Oltra-Carrió, R., Sobrino, J. A., Franch, B., & Nerry, F. (2012). Land surface emissivity retrieval from airborne sensor over urban areas. *Remote Sensing of Environment*, *123*, 298–305. https://doi.org/10.1016/j.rse.2012.03.007

Rajasekar, U., & Weng, Q. (2009). Urban heat island monitoring and analysis using a non-parametric model: A case study of Indianapolis. *ISPRS Journal of Photogrammetry and Remote Sensing*, *64*(1), 86–96. https://doi.org/10.1016/j.isprsjprs.2008.05.002

Ren, Y., Deng, L. Y., Zuo, S. Di, Song, X. D., Liao, Y. L., Xu, C. D., … Li, Z. W. (2016). Quantifying the influences of various ecological factors on land surface temperature of urban forests. *Environmental Pollution*, *216*, 519–529. https://doi.org/10.1016/j.envpol.2016.06.004

Shaker, R. R., Altman, Y., Deng, C., Vaz, E., & Forsythe, K. W. (2019). Investigating urban heat island through spatial analysis of New York City streetscapes. *Journal of Cleaner Production*, *233*, 972–992. https://doi.org/10.1016/j.jclepro.2019.05.389

Shirani-bidabadi, N., Nasrabadi, T., Faryadi, S., Larijani, A., & Shadman Roodposhti, M. (2019). Evaluating the spatial distribution and the intensity of urban heat island using remote sensing, case study of Isfahan city in Iran. *Sustainable Cities and Society*, *45*(December 2018), 686–692. https://doi.org/10.1016/j.scs.2018.12.005

Sobrino, J. A., Oltra-Carrió, R., Jiménez-Muñoz, J. C., Julien, Y., Sòria, G., Franch, B., & Mattar, C. (2012). Emissivity mapping over urban areas using a classification-based approach: Application to the Dual-use European Security IR Experiment (DESIREX). *International Journal of Applied Earth Observation and Geoinformation*, *18*(1), 141–147. https://doi.org/10.1016/j.jag.2012.01.022

Susca, T., Gaffin, S. R., Dell'Osso, G. R., Nakayama, T., Hashimoto, S., Tayyebi, A. A. H., … Stewart, I. D. (2018). Reducing Urban Heat Islands: Compendium of Strategies. *Sustainable Cities and Society*, *24*(1), 39p. https://doi.org/10.1016/j.uclim.2017.02.004

Weng, Q., Lu, D., & Schubring, J. (2004). Estimation of land surface temperature-vegetation abundance relationship for urban heat island studies. *Remote Sensing of Environment*, *89*(4), 467–483. https://doi.org/10.1016/j.rse.2003.11.005

Wu, Z., & Zhang, Y. (2019). *Water Bodies ' Cooling Effects on Urban Land Daytime Surface Temperature : Ecosystem Service Reducing Heat Island Effect*. 1–11. https://doi.org/10.3390/su11030787

Xiao, X. D., Dong, L., Yan, H., Yang, N., & Xiong, Y. (2018). The influence of the spatial characteristics of urban green space on the urban heat island effect in Suzhou Industrial Park. *Sustainable Cities and Society*, *40*(April 2017), 428–439. https://doi.org/10.1016/j.scs.2018.04.002